**This document is downloaded from DR-NTU (https://dr.ntu.edu.sg)
Nanyang Technological University, Singapore.**

Electrochemical deposition of Cl-doped n-type Cu2O on reduced graphene oxide electrodes

Wu, Shixin; Yin, Zongyou; He, Qiyuan; Lu, Gang; Zhou, Xiaozhu; Zhang, Hua

2011

Wu, S., Yin, Z., He, Q., Lu, G., Zhou, X., & Zhang, H. (2011). Electrochemical deposition of Cl-doped n-type Cu2O on reduced graphene oxide electrodes. Journal of Materials Chemistry, 21, 3467-3470.

https://hdl.handle.net/10356/94380

https://doi.org/10.1039/c0jm02267e

© 2011 The Royal Society of Chemistry. This is the author created version of a work that has been peer reviewed and accepted for publication by Journal of Materials Chemistry, The Royal Society of Chemistry. It incorporates referee’ s comments but changes resulting from the publishing process, such as copyediting, structural formatting, may not be reflected in this document. The published version is available at: http://dx.doi.org/10.1039/c0jm02267e.

Downloaded on 26 Aug 2022 02:53:35 SGT

Journal of
Materials Chemistry

Dynamic Article Links

Cite this: DOI: 10.1039/c0xx00000x

www.rsc.org/xxxxxx

ARTICLE TYPE

Electrochemical deposition of Cl-doped n-type Cu_2O on reduced graphene oxide electrodes†

Shixin Wu,[a] Zongyou Yin,[a] Qiyuan He,[a] Gang Lu,[a] Xiaozhu Zhou[a] and Hua Zhang*[ab]

Received (in XXX, XXX) Xth XXXXXXXXX 20XX, Accepted Xth XXXXXXXXX 20XX
DOI: 10.1039/b000000x

Reduced graphene oxide (rGO) electrodes can be applied for the electrochemical deposition of various semiconductor oxides. In this study, we demonstrate the electrochemical deposition of Cl-doped n-type Cu_2O (Cl–Cu_2O) on rGO electrodes. The structure and properties of the deposited Cl–Cu_2O have been investigated extensively. Moreover, the effect of Cl doping on the carrier concentration and photocurrent of Cl–Cu_2O has also been investigated. Our study shows significant implications in tailoring the properties of materials deposited on rGO electrodes by using electrochemical methods.

1. Introduction

Cuprous oxide (Cu_2O) is widely recognized as a p-type semiconductor oxide with a direct band gap of *ca.* 2.0 eV.[1] As an abundant and nontoxic material with high solar absorbance,[2,3] Cu_2O is promising for photovoltaic device applications.[4] A number of methods have been applied to synthesize Cu_2O, including the sol–gel chemistry approach,[5] various oxidation methods,[6] chemical vapor deposition,[7] and electrochemical deposition.[1–4,6,8] Among them, the electrochemical method has attracted increasing interest due to its characteristics of low temperature, low cost and large scale production, and also its facility to control morphologies, compositions and other element doping for the deposited materials.[2,9,10]

To date, extensive efforts have been tried to develop the solar cells based on the environmentally friendly material Cu_2O.[1,11,12] However, the conversion efficiency of the fabricated solar cells is lower than 2%.[13] One of the reasons for this is that it is difficult to prepare high quality n-type doped Cu_2O and construct Cu_2O p–n homojunctions.[14] Doping through introduction of a new element has been commonly used as a feasible way to tailor the electrical properties of metal oxides.[15] Although the pH value of solution was used to adjust the conduction type of Cu_2O, the resulting n-type Cu_2O showed high resistance of up to 10^8 Ω cm and poor performance in solar cell applications.[16]

Graphene, as a rising star in materials science, has been used for various applications such as field effect transistors (FETs),[17–19] sensors,[20–23] and memories,[24–27] due to its electronic properties.[28,29] In particular, graphene shows great potential as a transparent electrode material to compete with indium tin oxide (ITO) and fluorine tin oxide (FTO) for applications in photovoltaic devices.[30,31] In this study, by using the electrochemical method, we deposit high-quality n-type doped Cu_2O by introducing substitutional n-type dopant Cl on the reduced graphene oxide electrode (rGO), derived from chemical reduction of graphene oxide (GO).[32] Our results suggest that the deposition conditions have a great impact on the carrier concentration and the light harvesting efficiency of Cl-doped Cu_2O.

2. Experimental

2.1 Materials

Natural graphite (SP-1, Bay Carbon, Bay City, MI, USA) was purchased for synthesis of graphite oxide. Concentrated sulfuric acid (98% H_2SO_4), phosphorus oxide (P_2O_5), potassium peroxodisulfate ($K_2S_2O_8$), potassium permanganate ($KMnO_4$), hydrogen peroxide (30% H_2O_2), 3-aminopropyltriethoxysilane (APTES), anhydrous hydrazine (98% N_2H_4), cupric sulfate ($CuSO_4$), cupric chloride ($CuCl_2$), lactic acid and sodium hydroxide (NaOH) were purchased from Sigma-Aldrich (Milwaukee, WI, USA) and used as received. Si/SiO_2 was purchased from Bonda Technology Pte Ltd (Singapore). Ultrapure Milli-Q water (Milli-Q System, Millipore, Billerica, MA, USA) was used in all experiments.

2.2 Electrochemical deposition of Cl-doped Cu_2O (Cl–Cu_2O) on rGO electrodes

Graphene oxide (GO) in methanol solution was prepared according to the previous reports.[19,21] GO films were obtained by spin-coating GO methanol solution (0.5 mg mL^{-1}) on

[a] *School of Materials Science and Engineering, Nanyang Technological University, 50 Nanyang Avenue, Singapore, 639798, Singapore; Web: http://www.ntu.edu.sg/home/hzhang/; E-mail: HZhang@ntu.edu.sg; hzhang166@yahoo.com*
[b] *Center for Biomimetic Sensor Science, Nanyang Technological University, 50 Nanyang Drive, Singapore, 637553, Singapore*
† Electronic supplementary information (ESI) available: Characterizations of the rGO films and the MS plot of undoped Cu_2O. See DOI: 10.1039/c0jm02267e

APTES-modified SiO_2 substrates[21] at 4000 rpm, followed by reduction in hydrazine vapor at 60 °C overnight. The obtained rGO film was used as an electrode. The electrochemical deposition of Cl–Cu_2O was performed using an electrochemical workstation (CHI600C, CH Instrument Inc., USA) using the reported method.[16] Briefly, the deposition was carried out in a three-electrode electrochemical cell. The rGO electrode, a Pt mesh, and a saturated calomel electrode (SCE) were used as the working, counter and reference electrodes, respectively. The 10.67 mL electrolyte contained 0.3 M $CuSO_4$ and 4 M lactic acid. $CuCl_2$, with its amount varying from 0 to 1.6 mmol, was added into the electrolyte for Cl doping. After that, 4 M NaOH was added into the electrolyte to adjust the pH value of the solution to 8.0 ± 0.2. The deposition used a potentiostatic process (potential of −0.4 V, charge density of 2 C cm^{-2}) at a temperature of 60 °C.

2.3 Characterization

X-ray diffraction (XRD) patterns were recorded using an X-ray diffractometer (Rigaku D/max 2250 V) using Cu Kα radiation (λ = 1.5406 Å). Atomic force microscopy (AFM) image was obtained by using a Dimension 3100 (Veeco, CA, USA) with a Si tip (resonance frequency: 320 kHz; spring constant: 42 N m^{-1}) in tapping mode under ambient conditions (scanning rate: 1 Hz; scanning line: 512). Raman spectra were recorded with a WITec CRM200 confocal Raman microscopy system with an air cooling charge coupled device (CCD) as the detector (WITec Instruments Corp, Germany). The excitation wavelength was 488 nm. Scanning electron microscopy (SEM) images were obtained on a JEOL JSM-6340F field-emission scanning electron microanalyzer at an accelerating voltage of 5 kV. X-ray photoelectron spectroscopy (XPS) (AXIS ultra spectrometer, Kratos) spectra were collected with monochromatized Al Kα X-rays (1486.71 eV) and an operating power of 150 W (15 kV and 10 mA). Transmission electron microscopy (TEM) images were acquired on a JEOL JEM-2100F transmission electron microscope with an accelerating voltage of 200 kV. The TEM samples were prepared as follows. After the Cl–Cu_2O, deposited on rGO electrodes, was scratched with a needle, it was dispersed in water with sonication. 2 µL of this solution was dropped onto a copper grid. After the solution was dried, the sample was immediately used for TEM measurements. The Mott–Schottky (MS) plot was recorded by the electrochemical workstation using the ac impedance method. The measurement was conducted in a conventional three-electrode cell, using the rGO electrode with deposited Cl–Cu_2O, a saturated calomel electrode (SCE) and a Pt mesh as the working, reference and counter electrodes, respectively. The MS plots of Cl–Cu_2O were measured in the electrolyte containing 0.1 M Na_2HPO_4 with the solution pH adjusted to 10 ± 0.2 with 4 M NaOH (amplitude of the ac potential: 5 mV, frequency: 1 kHz). The photocurrent measurements were conducted in a three-electrode electrochemical cell with a 150 W halogen lamp irradiating the working electrode (with an area of *ca.* 0.3 cm^2). The rGO electrode with deposited Cl–Cu_2O, a standard saturated Ag/AgCl and a Pt wire were used as the working, reference and counter electrodes, respectively. The electrolyte contained 0.5 M Na_2SO_4.

3. Results and discussion

The electrochemical reactions involved in the synthesis can be expressed by two equations:[14] $Cu^{2+} + e^- \rightarrow Cu^+$ and $2Cu^+ + 2OH^- \rightarrow Cu_2O + H_2O$. With the addition of $CuCl_2$ into the electrolyte, another reaction is expected to occur:[16] $Cu^+ + Cl^- \rightarrow CuCl$. The expected electrochemical reaction and the limited solubility of CuCl induce the incorporation of Cl into Cu_2O lattice.[16] Since the radius of Cl^- ions (1.8 Å) is larger than that of O^{2-} ions (1.4 Å), doping of Cl is usually substitutional.

A typical sample of n-type Cu_2O was deposited on the rGO electrode, which was characterized by AFM, SEM and Raman (Fig. 1S in ESI†), in 10.67 mL electrolyte containing 0.3 M $CuSO_4$, 4 M lactic acid, and 1 mmol $CuCl_2$. The obtained product is referred to as Cl–Cu_2O, and was fully characterized as discussed below. The XRD pattern (Fig. 1A) confirms the successful synthesis of Cu_2O and no other phases were formed even with Cl doping, indicating the cubic crystal structure of Cl–Cu_2O with space group of $Pn\bar{3}$.[6] The narrow diffraction peaks suggest the good crystallinity of the electrodeposited Cl–Cu_2O.

Fig. 1B displays the Raman spectrum of Cl–Cu_2O deposited on rGO film. The strongest peak in the spectrum is from the SiO_2 substrate, whose peak at 520 cm^{-1} was used as calibration. Peaks at 1360 and 1594 cm^{-1} belong to the D and G band of rGO electrodes, respectively.[33] Peaks at lower wavenumbers, 218, 306, 435 and 625 cm^{-1}, correspond to the second-order overtones 2 $\Gamma\overline{12}$, 2 $\Gamma_{15}^{(1)}$, fourth-order overtone 4 $\Gamma\overline{12}$, red-allowed mode $\Gamma_{15}^{(2)}$ (TO) phonon vibration of crystalline Cu_2O,[34] respectively. The peak at 980 cm^{-1} is most likely the overlapping peak of SiO_2 substrate and the adsorbed sulfate species on Cu_2O crystals since the electrolyte used for Cl–Cu_2O deposition contained $CuSO_4$.[35]

Fig. 2A shows the SEM image of the Cl–Cu_2O and the inset exhibits an enlarged view. Besides the micrometre sized crystals with typical (111) planes at the sides, multifaceted crystals nucleated on the pre-formed crystals are also observed. EDX spectrum (Fig. 2B) shows the elemental composition of Cl–Cu_2O and confirms the incorporation of Cl into the synthesized Cu_2O. The atomic concentration of Cl is estimated to be 2.1% from the EDX quantitative analysis. Moreover, the X-ray photoelectron spectrum (XPS) of the sample also confirmed the presence of Cl in the electrodeposited Cu_2O (data not shown here). TEM image of a Cl–Cu_2O crystal scratched from the electrodeposited Cl–Cu_2O on the rGO electrode is shown in Fig. 2C. The selected area electron diffraction (SAED) pattern (inset in Fig. 2C) from the crystal displays clearly resolved diffraction dots, indicating the high crystallinity of the deposited Cl–Cu_2O on the rGO electrode.

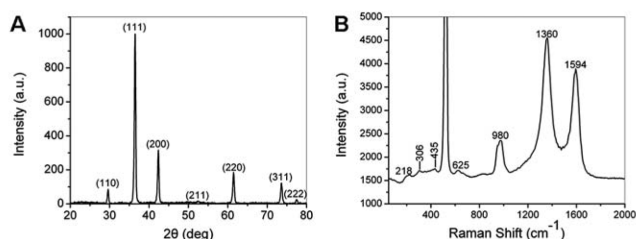

Fig. 1 (A) XRD pattern and (B) Raman spectrum of Cl–Cu_2O deposited on rGO electrode.

This journal is © The Royal Society of Chemistry [year]

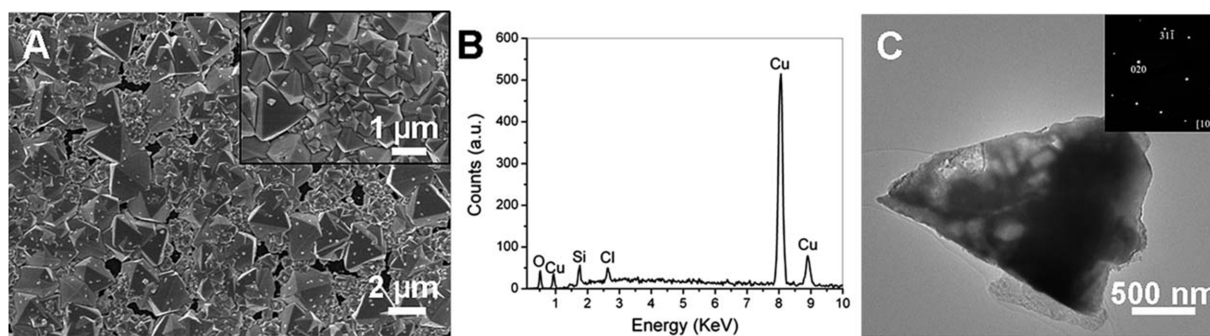

Fig. 2 (A) SEM image and (B) EDX spectrum of electrochemically deposited Cl–Cu_2O on rGO electrode. (C) TEM image of a Cl–Cu_2O crystal. Inset: SAED pattern.

The conduction type and carrier concentration of Cl–Cu_2O were determined using Mott–Schottky (MS) measurements. The MS plot (Fig. 3A) of the sample shows a positive slope, which confirms the n-type semiconducting behavior of Cl–Cu_2O. The donor concentration calculated from the slope of the plot using the MS theory[14] is about 1×10^{20} cm^{-3} (6.3 is used as the dielectric constant of Cu_2O).

To study the effect of chlorine precursor ($CuCl_2$) on the carrier concentration of Cu_2O film, a series of samples were deposited in the electrolyte containing different $CuCl_2$ amounts. All the samples exhibited a positive slope in the MS plot and hence n-type semiconducting behavior. The change of doping concentration with the amount of $CuCl_2$ added into the solution is shown in Fig. 3B. Doping concentration increases slowly with addition of $CuCl_2$ until the amount of $CuCl_2$ is 1.0 mmol, after that the doping concentration decreases rapidly. Theoretically, Cl (group VII element), as a substitutional dopant for O (group VI element) site in Cu_2O, would contribute electrons to the crystal, hence increasing the electron (donor) concentration of Cu_2O.

However, in our experiments, when the amount of $CuCl_2$ exceeds 1.0 mmol, it becomes difficult to electrodeposit Cu_2O crystals. The amount of Cl–Cu_2O crystals on the rGO electrode deposited with the addition of 1.3 mmol $CuCl_2$ is much lower compared to those deposited with the addition of 0.3 and 1.0 mmol $CuCl_2$ (as shown in Fig. 4). This could be explained by the inhibition effect of Cl^- ions during the electrodeposition of Cu caused by the surface covered with almost insoluble CuCl.[36] Moreover, kinetics and mechanisms of Cu deposition are

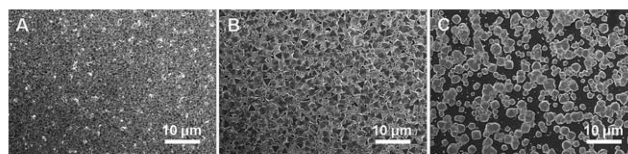

Fig. 4 SEM images of electrochemically deposited Cl–Cu_2O with addition of (A) 0.3, (B) 1.0, and (C) 1.3 mmol $CuCl_2$.

changed with increased anodic exchange current density when the Cl^- ion concentration is above 8.45×10^{-4} M.[36]

Fig. 5 displays the photocurrent measurements on three samples of Cl–Cu_2O deposited with different amounts of chlorine precursor. The measurements were conducted in a solution of 0.5 M Na_2SO_4 at an applied potential of −0.5 V (*vs.* Ag/AgCl). Anodic photocurrents, characteristics of n-type semiconducting material,[16] were observed for all the samples. Clearly, Cl–Cu_2O deposited with the addition of 0.3 mmol (referred to as 0.3–Cl–Cu_2O) and 1.0 mmol $CuCl_2$ (referred to as 1.0–Cl–Cu_2O) shows much higher light-to-electrons/holes conversion efficiency, thus larger photocurrent, than that deposited with the addition of 1.3 mmol $CuCl_2$ (referred to as 1.3–Cl–Cu_2O). It is believed that the surface coverage of the deposited Cl–Cu_2O on the rGO electrode is the main factor that influences the light harvesting efficiency. Fig. 4 clearly shows that the surface coverage of 0.3–Cl–Cu_2O and 1.0–Cl–Cu_2O is larger than that of 1.3–Cl–Cu_2O. The slightly higher photocurrent from 1.0–Cl–Cu_2O, compared with 0.3–Cl–Cu_2O, can be attributed to the higher Cl-doping

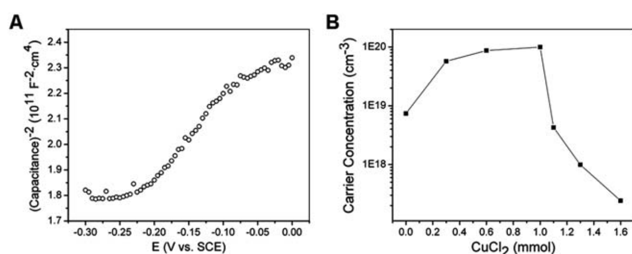

Fig. 3 (A) Mott–Schottky plot of Cl–Cu_2O on rGO electrode measured in 0.1 M Na_2HPO_4 solution at pH 10. (B) Variation of carrier concentration as a function of the amount of $CuCl_2$ added into the electrolyte. As a reference, when the amount of $CuCl_2$ is 0 mmol, the MS plot for the undoped n-type Cu_2O is shown in Fig. 2S in ESI.†

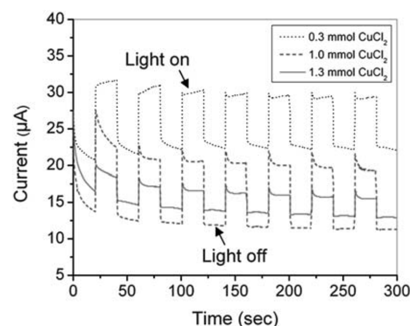

Fig. 5 Photocurrent measured from Cl–Cu_2O with three different chlorine precursor amounts.

concentration in 1.0–Cl–Cu_2O although the surface coverage of these two Cu_2O crystals on rGO electrode is similar.

4. Conclusions

In summary, n-type Cu_2O by Cl doping with carrier concentration of up to 1×10^{20} cm^{-3} has been electrodeposited on rGO electrodes. Through various characterizations, a comprehensive understanding about the structure and properties of the deposited Cl–Cu_2O was obtained. Furthermore, the amount of chlorine precursor in the electrolyte has been found to have a direct impact on the surface coverage of deposited Cu_2O crystals on the rGO electrode, subsequently affecting the Cl-doping concentration and light harvesting efficiency of Cl–Cu_2O. Our study has explored rGO-based electrochemical synthesis and promises the potential for various future applications in optoelectronic devices based on rGO electrodes.

Acknowledgements

This work was supported by AcRF Tier 2 (ARC 10/10, No. MOE2010-T2-1-060) from MOE, A*STAR SERC Grant (No. 092 101 0064) from A*STAR, and the Centre for Biomimetic Sensor Science at NTU in Singapore.

Notes and references

1 K. H. Han and M. Tao, *Sol. Energy Mater. Sol. Cells*, 2009, **93**, 153.
2 S. Bijani, L. Martínez, M. Gabás, E. A. Dalchiele and J. R. Ramos-Barrado, *J. Phys. Chem. C*, 2009, **113**, 19482.
3 C. M. McShane and K. S. Choi, *J. Am. Chem. Soc.*, 2009, **131**, 2561.
4 L. C. Wang, N. R. de Tacconi, C. R. Chenthamarakshan, K. Rajeshwar and M. Tao, *Thin Solid Films*, 2007, **515**, 3090.
5 S. C. Ray, *Sol. Energy Mater. Sol. Cells*, 2001, **68**, 307.
6 T. D. Golden, M. G. Shumsky, Y. C. Zhou, R. A. VanderWerf, R. A. Van Leeuwen and J. A. Switzer, *Chem. Mater.*, 1996, **8**, 2499.
7 T. Maruyama, *Sol. Energy Mater. Sol. Cells*, 1998, **56**, 85.
8 S. X. Wu, Z. Y. Yin, Q. Y. He, X. Huang, X. Z. Zhou and H. Zhang, *J. Phys. Chem. C*, 2010, **114**, 11816.
9 J. Rousset, E. Saucedo and D. Lincot, *Chem. Mater.*, 2009, **21**, 534.
10 G. H. A. Therese and P. V. Kamath, *Chem. Mater.*, 2000, **12**, 1195.
11 B. D. Yuhas and P. Yang, *J. Am. Chem. Soc.*, 2009, **131**, 3756.
12 J. Katayama, K. Ito, M. Matsuoka and J. Tamaki, *J. Appl. Electrochem.*, 2004, **34**, 687.
13 A. Mittiga, E. Salza, F. Sarto, M. Tucci and R. Vasanthi, *Appl. Phys. Lett.*, 2006, **88**, 163502.
14 L. C. Wang and M. Tao, *Electrochem. Solid-State Lett.*, 2007, **10**, H248.
15 G. D. Yuan, W. J. Zhang, J. S. Jie, X. Fan, J. X. Tang, I. Shafiq, Z. Z. Ye, C. S. Lee and S. T. Lee, *Adv. Mater.*, 2008, **20**, 168.
16 X. F. Han, K. H. Han and M. Tao, *Electrochem. Solid-State Lett.*, 2009, **12**, H89.
17 J. Bai, X. Zhong, S. Jiang, Y. Huang and X. Duan, *Nat. Nanotechnol.*, 2010, **5**, 190.
18 K. S. Novoselov, A. K. Geim, S. V. Morozov, D. Jiang, Y. Zhang, S. V. Dubonos, I. V. Grigorieva and A. Firsov, *Science*, 2004, **306**, 666.
19 B. Li, X. H. Cao, H. G. Ong, J. W. Cheah, X. Z. Zhou, Z. Y. Yin, H. Li, J. Wang, F. Y. C. Boey, W. Huang and H. Zhang, *Adv. Mater.*, 2010, **22**, 3058.
20 Z. Wang, X. Zhou, J. Zhang, F. Boey and H. Zhang, *J. Phys. Chem. C*, 2009, **113**, 14071.
21 J. D. Fowler, M. J. Allen, V. C. Tung, Y. Yang, R. B. Kaner and B. H. Weiller, *ACS Nano*, 2009, **3**, 301.
22 Q. Y. He, H. G. Sudibya, Z. Y. Yin, S. X. Wu, H. Li, F. Boey, W. Huang, P. Chen and H. Zhang, *ACS Nano*, 2010, **4**, 3201.
23 S. He, B. Song, D. Li, C. Zhu, W. Qi, Y. Wen, L. Wang, S. Song, H. Fang and C. Fan, *Adv. Funct. Mater.*, 2010, **20**, 453.
24 X. Zhuang, Y. Chen, G. Liu, P. Li, C. Zhu, E. Kang, K. Noeh, B. Zhang, J. Zhu and Y. Li, *Adv. Mater.*, 2010, **22**, 1731.
25 J. Q. Liu, Z. Y. Yin, X. H. Cao, F. Zhao, A. Ling, L. H. Xie, Q. L. Fan, F. Boey, H. Zhang and W. Huang, *ACS Nano*, 2010, **4**, 3987.
26 S. Myung, J. Park, H. Lee, K. S. Kim and S. Hong, *Adv. Mater.*, 2010, **22**, 2045.
27 J. Q. Liu, Z. Lin, T. Liu, Z. Y. Yin, X. Z. Zhou, S. Chen, L. H. Xie, F. Boey, H. Zhang and W. Huang, *Small*, 2010, **6**, 1536.
28 A. K. Geim and K. S. Novoselov, *Nat. Mater.*, 2007, **6**, 183.
29 A. K. Geim, *Science*, 2009, **324**, 1530.
30 Z. Y. Yin, S. X. Wu, X. Z. Zhou, X. Huang, Q. C. Zhang, F. Y. C. Boey and H. Zhang, *Small*, 2010, **6**, 307.
31 Z. Y. Yin, S. Sun, T. Salim, S. X. Wu, X. Huang, Q. Y. He, Y. M. Lam and H. Zhang, *ACS Nano*, 2010, **4**, 5263.
32 X. Z. Zhou, X. Huang, X. Y. Qi, S. X. Wu, C. Xue, F. Y. C. Boey, Q. Y. Yan, P. Chen and H. Zhang, *J. Phys. Chem. C*, 2009, **113**, 10842.
33 S. Stankovich, D. A. Dikin, R. D. Piner, K. A. Kohlhaas, A. Kleinhammes, Y. Jia, Y. Wu, S. T. Nguyen and R. S. Ruoff, *Carbon*, 2007, **45**, 1558.
34 H. Solache-Carranco, G. Juárez-Díaz, A. Esparza-García, M. Briseño-García, M. Galván-Arellano, J. Martínez-Juárez, G. Romero-Paredes and R. J. Peña-Sierra, *J. Lumin.*, 2009, **129**, 1483.
35 F. Texier, L. Servant, J. L. Bruneel and F. Argoul, *J. Electroanal. Chem.*, 1998, **446**, 189.
36 Z. D. Stanković, *Electrochim. Acta*, 1984, **29**, 407.

This journal is © The Royal Society of Chemistry [year]